# Electrochemistry of Ruthenium Metallocenes. 1. Synthesis, NMR, and Anodic Electrochemical Behavior of Vinyl-Substituted Ruthenium Cyclophane Complexes

Bernhard Gollas and Bernd Speiser*

*Institut für Organische Chemie, Universität Tübingen, Auf der Morgenstelle 18, D-72076 Tübingen, Germany*

Jürgen Sieglen and Joachim Strähle

*Institut für Anorganische Chemie, Universität Tübingen, Auf der Morgenstelle 18, D-72076 Tübingen, Germany*

Ruthenium complexes of 4-ethenyl- and 4,12-diethenyl[2₂]paracyclophane have been synthesized and investigated by NMR spectroscopy as well as electroanalytical techniques. The structure of $[(C_{20}H_{20})Ru(II)(C_{16}H_{16})](BF_4)_2 \cdot (acetone)$ was determined by X-ray crystallography. Consistently, the results show that electron density is decreased in those ("disturbed") vinyl groups bound directly to ruthenium-complexed cyclophane decks. Electrochemical oxidation of the complexes depends on the presence or absence of undisturbed vinyl groups and results in the formation of redox-active films on the electrode.

## Introduction

Band structure calculations predict interesting electronic properties (e.g., electric conductivity) for stacked, columnar metallocene polymers.[1] Such materials have received increasing interest[2] due to their expected applications. In an attempt to find suitable model monomer units, Boekelheide and co-workers described the synthesis of mono- and diruthenium complexes of [2ₙ]cyclophanes and polycyclic arenes as well as their electrochemical and chemical reduction.[3−9]

*Mono*ruthenium(II) complexes of [2ₙ]cyclophanes (e.g., **1** and **2**) are reduced in a metal-centered overall two-electron process.[5] In the ruthenium(0) complexes formed, distortion of one of the ligands enables a hapticity change from $\eta^6$ to $\eta^4$, which allows the ruthenium atom to keep its 18-electron count.[6] Two-electron reduction of *di*ruthenium(II,II) complexes (e.g., **3**) depends on the geometry and rigidity of the [2ₙ]cyclophane ligands. It is either metal-centered, resulting in formation of a mixed-valence ion exhibiting an intramolecular net two-electron transfer,[7] or ligand-centered, converting the cyclophane to a system of two cyclohexadienyl anions joined by an extremely long carbon−carbon bond[8] (see, for example, step 3 in Scheme 1). In the former case, complete reduction to a diruthenium(0,0) complex can
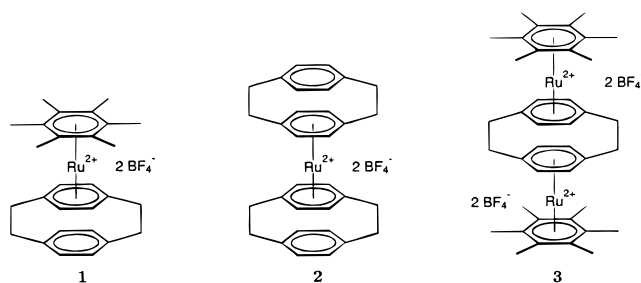


be achieved. Extended-Hückel MO calculations for a hypothetical oligomeric tetraruthenium homologue of one of the latter cases, with [2₂]paracyclophane as ligand, show that the bonding HOMO is delocalized over all ruthenium atoms and cyclophane units.[8] These unusual properties make polymeric materials based on such ruthenium−cyclophane subunits extremely attractive goals.

The most extended oligomer prepared with a defined structure was the triruthenium complex **4**.[6] Attempts
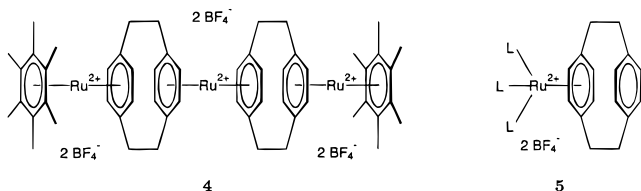


to enlarge this chain to the tetra- and pentaruthenium compounds, to higher oligomers, or polymers by thermal self-condensation of ([2₂]paracyclophane)ruthenium(II) tris(acetone) solvate **5** (L = acetone) resulted in inseparable mixtures of lower oligomers that could not be characterized unambiguously.[4,6] Possibly, the failure of these attempts is due to uncontrolled solvolysis equilibria.

Based on a recent proposal by Boekelheide and co-workers to prepare such materials by electrochemical

⊗ Abstract published in *Advance ACS Abstracts,* November 15, 1995.
(1) Burdett, J. K.; Canadell, E. *Organometallics* **1985,** *4,* 805−815.
(2) Rosenblum, M. *Adv. Mater.* **1994,** *6,* 159−162.
(3) Laganis, E. D.; Voegeli, R. H.; Swann, R. T.; Finke, R. G.; Hopf, H.; Boekelheide, V. *Organometallics* **1982,** *1,* 1415−1420.
(4) Rohrbach, W. D.; Boekelheide, V. *J. Org. Chem.* **1983,** *48,* 3673−3678.
(5) Finke, R. G.; Voegeli, R. H.; Laganis, E. D.; Boekelheide, V. *Organometallics* **1983,** *2,* 347−350.
(6) Swann, R. T.; Hanson, A. W.; Boekelheide, V. *J. Am. Chem. Soc.* **1986,** *108,* 3324−3334.
(7) Voegeli, R. H.; Kang, H. C.; Finke, R. G.; Boekelheide, V. *J. Am. Chem. Soc.* **1986,** *108,* 7010−7016.
(8) Plitzko, K.-D.; Rapko, B.; Gollas, B.; Wehrle, G.; Weakley, T.; Pierce, D. T.; Geiger, W. E.; Haddon, R. C.; Boekelheide, V. *J. Am. Chem. Soc.* **1990,** *112,* 6545−6556.
(9) Plitzko, K.-D.; Wehrle, G.; Gollas, B.; Rapko, B.; Dannheim, J.; Boekelheide, V. *J. Am. Chem. Soc.* **1990,** *112,* 6556−6564.

**Scheme 1. Proposed Approach for the Construction of Polymeric Cyclophane−Ruthenium Metallocenes.**
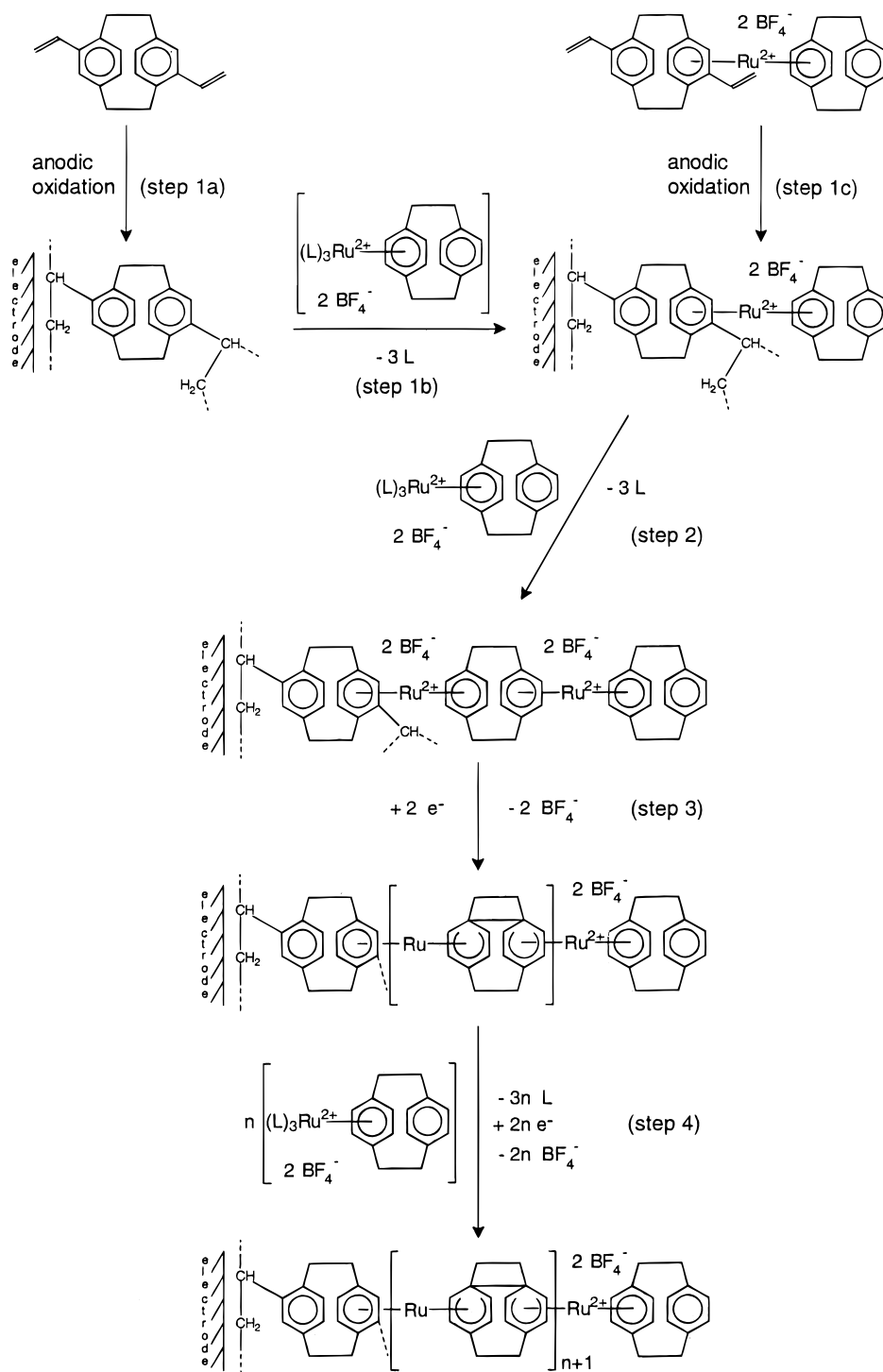


crystal growth,[8] an alternative route for the synthesis of metallocene polymers is introduced here (Scheme 1). Step 1 of this route involves chemical modification of an electrode to provide reaction and anchor sites for condensation of the monomeric solvates **5**. Subsequently, alternating thermal condensation and *in-situ* electrochemical reduction could lead to formation of polymeric metallocene stacks at the electrode (steps 2−4 in Scheme 1).

Reaction centers on an electrode surface for such an electrochemical "solid phase" synthesis may be created by deposition of a thin polymer film containing appropriate subunits. In analogy to the electropolymerization of styrene,[10,11] it may be possible to polymerize

vinyl-substituted cyclophanes by anodic oxidation (step 1a in Scheme 1). The resulting polymer film may be functionalized by capping with solvates such as **5** (step 1b). Alternatively, vinylcyclophanes could be used as ligands in ruthenium complexes. If such vinyl-substituted complexes polymerize upon electrooxidation, it might be possible to accomplish steps 1a and 1b in Scheme 1 in a single reaction (step 1c). This first part of the synthesis should produce a redox-active polymer film attached to the electrode surface. Now, capping of

(10) Akbulut, U.; Fernandez, J. E.; Birke, R. L. *J. Polym. Sci., Polym. Chem. Ed.* **1975**, *13*, 133−149.

(11) Garg, B. K.; Raff, R. A. V.; Subramanian, R. V. *J. Appl. Polym. Sci.* **1978**, *22*, 65−87.

metallocenes in the film (step 2) would result in diruthenium units. In analogy to **3**, they may likewise be reduced under formation of a new carbon−carbon bond (step 3). Repetition of these two reaction steps could then lead to metallocene polymers (step 4).

Possibly, reduced intermediate oligomers on the electrode have a higher tendency toward chain growth than the initially formed (oxidized) oligomers. The lower positive charge should result in decreased Coulombic repulsion between immobilized oligomers and the diffusing solvates and also in higher electron density at the reaction centers of the respective chain ends. Hence, *in-situ* electrochemical reduction could be a tool to control the aforementioned solvolysis equilibria and to shift them toward formation of polymeric stacks at the electrode.

The present paper reports on the syntheses of ruthenium complexes derived from vinylcyclophanes and the investigation of their structure and electrochemical behavior, including their electropolymerization under formation of redox-active films.

## Results and Discussion

**Syntheses.** Syntheses of 4-ethenyl[2$_2$]paracyclophane (**6**) and 4,12-diethenyl[2$_2$]paracyclophane (**7**) have been described by Hopf and co-workers,[12] and these compounds were used as ligands for the ruthenium complexes in the present work.
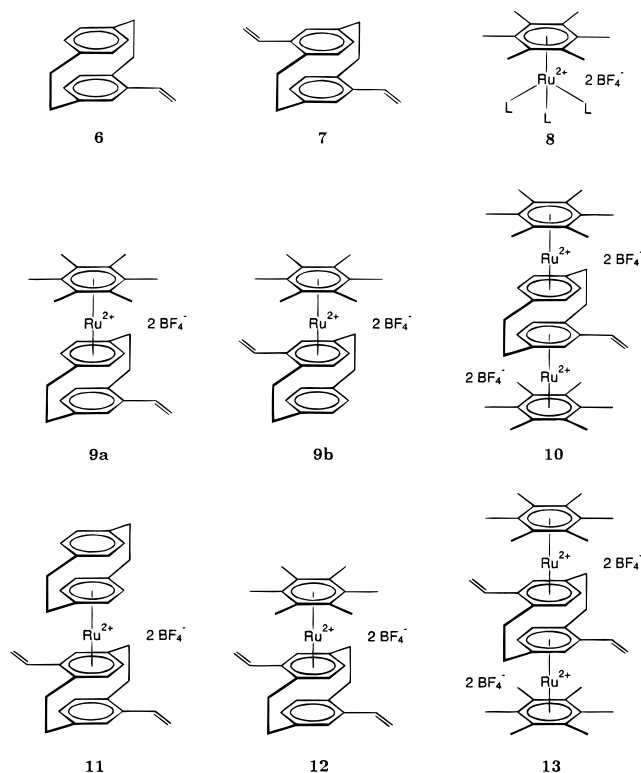


A synthetic procedure for the preparation of bis-(arene)ruthenium(II) sandwich complexes was initially developed by Bennett.[13,14] It was successfully employed

to prepare ruthenium(II) complexes of [2$_n$]cyclophanes[3] and slightly modified to increase the yields of cyclophane and arene diruthenium(II,II) complexes.[8] Monoruthenium(II) cyclophane complexes without vinyl groups, e.g., **1** and **2**, were prepared by heating of the [2$_n$]-cyclophane in a solution of the appropriate arene− or cyclophane−ruthenium solvate in the presence of trifluoroacetic acid (TFA).[6] Treatment with a 10-fold excess of the hexamethylbenzene−ruthenium solvate **8** led to the biscapped cyclophane complexes,[8] e.g., **3**.

Application of these conditions to the reaction of **6** with **8** did not yield the desired analogous monocapped (vinylcyclophane)ruthenium complex. Instead, a nonuniformly colored solid was obtained, whose $^1$H NMR spectrum showed a multitude of signals in the region of the aromatic, the methylene, and the hexamethylbenzene protons. Apparently, heating of vinylcyclophanes in TFA leads to partial polymerization. This was confirmed by $^1$H and $^{13}$C NMR spectra of the product obtained by reaction of **6** in neat refluxing TFA. The signals of the vinyl groups disappear, and the aromatic and the methylene region of the spectra show broad humps consisting of numerous overlapping signals. The IR spectrum (KBr pellet) shows the absence of the typical band for the stretching frequency of the vinylic double bond in the monomer at 1620 cm$^{-1}$.

The capping reaction, however, also works without TFA as catalyst, although slower and with decreased yields as compared to the synthesis of **1**−**3** with the acid. With this modified procedure and acetone as solvent, complexes **9**−**13** could be prepared in moderate to good yields. The monocapping reaction of **6** with **8** gave a 2:1 mixture of the isomers **9a** and **9b** due to the presence of a substituted and an unsubstituted aromatic deck. The isomers could not be separated. Biscapping to **10** and **13** was achieved by employing a 10-fold excess of the hexamethylbenzene−ruthenium solvate.

Since we started from a racemic mixture of the chiral ligand **6**, complexes **9a**, **9b**, and **10** consist of mixtures of the corresponding enantiomers. 4,12-Diethenyl[2$_2$]-paracyclophane (**7**) on the other hand is achiral. In this case, monocapping of **7** with **5** or **8** produces racemates of **11** and **12** by reduction of the symmetry of the molecule. Biscapped compound **13**, however, is again achiral. Although separation of enantiomers of [2$_2$]-paracyclophane derivatives by chromatographic methods has been described,[15,16] such a separation was not attempted for the complexes prepared in the present work.

**Crystal Structure of 11.** Crystals of **11** suitable for a single-crystal X-ray structure analysis were prepared by the vapor diffusion technique (see Experimental Section). Figure 1 shows Schakal computer projections of the structure of the 12*R* enantiomer in the solid state (Tables 3 and 4 show the 12*S* enantiomer). The unit cell contains a molecule of the 12*R* and the 12*S* enantiomer each. Table 1 lists the crystal and refinement data, while Table 2 gives selected interatomic and mean plane distances together with selected angles between bonds and mean planes.

Although X-ray crystallographic structures of some (hexamethylbenzene)(cyclophane)ruthenium complexes

(12) Herrmann, E. Dissertation, Technische Universität Braunschweig, Braunschweig, Germany, 1990.
(13) Bennett, M. A.; Huang, T.-N.; Matheson, T. W.; Smith, A. K. *Inorg. Synth.* **1982**, *21*, 74−78.
(14) Bennett, M. A.; Matheson, T. W. *J. Organomet. Chem.* **1979**, *175*, 87−93.

(15) Hopf, H.; Grahn, W.; Barrett, D. G.; Gerdes, A.; Hilmer, J.; Hucker, J.; Okamoto, Y.; Kaida, Y. *Chem. Ber.* **1990**, *123*, 841−845.
(16) König, W. A.; Gehrcke, B.; Hochmuth, D. H.; Mlynek, C.; Hopf, H. *Tetrahedron Asymmetry* **1994**, *5*, 347−350.
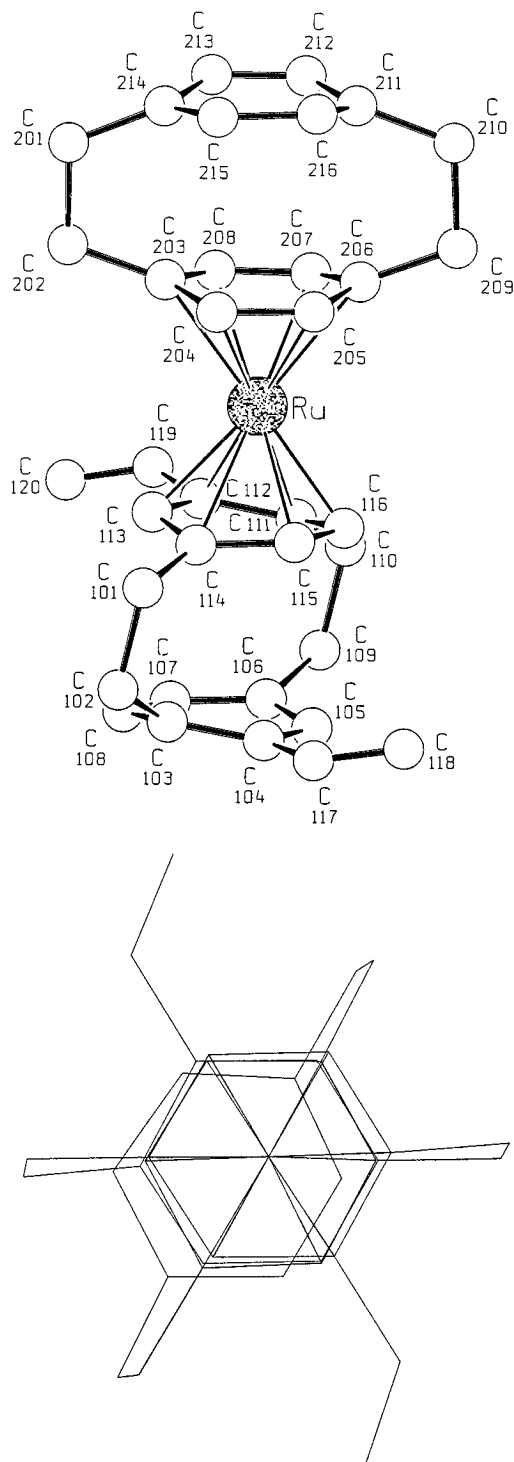
**Figure 1.** Structure of (12*R*)-($\eta^6$-[2$_2$](1,4)cyclophane)(11-16-$\eta^6$-4,12-diethenyl[2$_2$](1,4)cyclophane)ruthenium(II) bis(tetrafluoroborate)·$C_3H_6O$ (**11**): (a, top) side view of the complex and (b, bottom) top view, showing relative conformation of the two cyclophane ligands.

have been discussed previously,[6,17] this is the first structure of a bis([2$_n$]cyclophane)ruthenium complex determined by X-ray crystallography. Both cyclophane ligands are bound $\eta^6$ to ruthenium as are the bis(arene)-ruthenium(II)[18] and (arene)(cyclophane)ruthenium(II)[17] complexes. Both ligands retain the boat-shaped geometry of the cyclophane decks[19] in the complex. Hence,

(17) Hanson, A. W. *Cryst. Struct. Commun.* **1982**, *11*, 1019−1026.
(18) Suravajjala, S.; Polam, J. R.; Porter, L. C. *Organometallics* **1994**, *13*, 37−42.

### Table 1. Crystallographic Data for 11

| | |
|---|---|
| empirical formula | $C_{39}H_{42}B_2F_8ORu$ |
| fw | 801.42 |
| temp (K) | 213(2) |
| wavelength (Å) | 0.709 30 |
| crystal system | triclinic |
| space group | $P\bar{1}$ |
| unit cell dimension | |
| $a$ (Å) | 8.752(4) |
| $b$ (Å) | 12.809(6) |
| $c$ (Å) | 16.211(8) |
| $\alpha$ (deg) | 86.30(3) |
| $\beta$ (deg) | 86.53(3) |
| $\gamma$ (deg) | 77.15(4) |
| $V$ (Å$^3$) | 1766.2(14) |
| $Z$ | 2 |
| density$_{cald}$ (Mg/m$^3$) | 1.507 |
| absrptn coeff (mm$^{-1}$) | 0.518 |
| $F(000)$ | 820 |
| crystal size (mm) | 0.4 × 0.25 × 0.05 |
| $\theta$ range (deg) | 3.07−23.96 |
| index ranges | $-1 \le h \le 10$, $-14 \le k \le 14$, $-18 \le l \le 18$ |
| no. of reflctns measd | 6744 |
| no. of unique reflctns | 4660 |
| refined parameters | 460 |
| refinement method | full-matrix least squares on $F^2$ |
| final $R$ indices$^a$ ($I > 2\sigma(I)$) | $R_1 = 0.0719$, $wR_2 = 0.1800$ |
| goodness of fit$^b$ on $F^2$ | 1.086 |
| largest diff peak and hole (e/Å$^{-3}$) | 1.727 and −1.653 |

$^a$ $R_1 = [\sum||F_o| - |F_c||]/\sum|F_o|$ (based on $F$); $wR_2 = [[\sum w(|F_o - F_c|)^2]/[\sum w(|F_o|^2)]]^{1/2}$ (based on $F^2$). $w = q/[(\sigma F_o)^2 + (aP)^2 + bP + d + e\sin\theta]$. $^b$ Goodness of fit, $[\sum w(|F_o^2| - |F_c^2|)^2/(N_{obs} - N_{params})]^{1/2}$.

### Table 2. Selected Angles and Distances for 11

| Angles between Mean Planes (deg) | |
|---|---|
| C(112,119,120)−C(111−116) | 23.8(1.1) |
| C(104,117,118)−C(103−108) | 16.8(1.1) |
| C(111−116)−C(103−108) | 1.2(2) |
| C(111−116)−C(203−208) | 4.6(4) |
| C(203−208)−C(211−216) | 0.6(4) |
| C(101,103,106,109,110,111,114)−C(201−203,206,209,210,211,214) | 57.6(3) |

| Distances between Atoms and Mean Planes (Å) | | | |
|---|---|---|---|
| C(112)−C(119) | 1.466(10) | C(111−116)−Ru | 1.752(3) |
| C(104)−C(117) | 1.463(11) | C(211−216)−Ru | 4.626(4) |
| C(119)−C(120) | 1.316(12) | C(103−108)−Ru | 4.625(4) |
| C(117)−C(118) | 1.330(13) | C(203−208)−Ru | 1.753(3) |
| Ru−C(111) | 2.366(6) | Ru−C(206) | 2.356(8) |
| Ru−C(112) | 2.215(6) | Ru−C(207) | 2.185(7) |
| Ru−C(113) | 2.170(7) | Ru−C(208) | 2.182(7) |
| Ru−C(114) | 2.319(6) | Ru−C(203) | 2.298(7) |
| Ru−C(115) | 2.183(6) | Ru−C(204) | 2.148(7) |
| Ru−C(116) | 2.190(6) | Ru−C(205) | 2.192(8) |

the bond distances between the ruthenium atom and the bridgehead carbons are longer than those between ruthenium and the other carbons of the two complexed cyclophane decks (Table 2). There is no direct bonding interaction between the vinyl groups and the metal. The presence of the two vinyl substituents, however, results in small deviations from the ideal metallocene structure. The ruthenium-bound decks of the two cyclophane ligands are not completely coplanar. Their mean planes are tilted by an angle of 4.6°, which may be attributed to steric interactions between the vinyl group at C(12) and the ruthenium atom. The four cyclophane decks are arranged in an eclipsed conformation, whereas the two ethano bridges of the unsubstituted cyclophane ligand occupy staggered positions with respect to the bridges and vinyl groups of the substituted ligand (Figure 1b). Mean plane distances between the ruthe-

(19) Brown, C. J. *J. Chem. Soc.* **1953**, 3265−3270.

nium atom and the two inner and the two outer decks, respectively, are equal. Due to relatively large statistical errors in the determination of the positions of C(17), C(18), C(19), and C(20), no reliable information about possible differences in bond lengths for the two vinyl groups as a consequence of electronic effects discussed in the NMR section is available.

**NMR Spectral Analysis.** In previous studies of ruthenium cyclophane complexes, the Ru(II) species had all been characterized by their ^{1}H NMR spectra;[3,4,6,7] for a few of them ^{13}C NMR data were also reported.[4] Due to the high symmetry of the molecules, the aromatic protons showed very simple spin systems.

In the case of the vinyl-substituted compounds discussed here, the spectra are more complex. The derivatives of **6** are lacking any symmetry elements, which leads to complicated ^{1}H NMR spectra, whereas the complexes of the centrosymmetric **7** show somewhat simpler spectra. The ^{1}H and ^{13}C NMR spectra of the new complexes were interpreted as completely as possible.

The spin systems in the ^{1}H NMR spectra were analyzed by means of two-dimensional H,H-COSY experiments. With these results it was possible to determine connectivities from two-dimensional C,H-COSY experiments and to assign the ^{13}C signals to the individual primary, secondary, and tertiary carbons. Two-dimensional long-range C,H-COSY experiments then allowed the assignment of signals to the remaining quaternary carbons. Tables 3 and 4 summarize the ^{1}H and the ^{13}C NMR spectral properties of the free cyclophane ligands **6** and **7** and the complexes **9−13**.

**^{1}H NMR Spectra.** The spectrum of the cyclophane ligand **6** is composed of five different spin systems: those of the vinyl group, the substituted and the unsubstituted aromatic deck, and the two different ethano bridges. The spectrum of the pseudo-para-disubstituted cyclophane **7** is simplified to three spin systems with equivalent vinyl groups, aromatic decks, and ethano bridges, respectively. The systems of the aromatic and the ethenyl protons appeared to be first order under the applied field strength for all compounds. The spin systems of the protons in the ethano bridges could, however, only be resolved in the spectrum of **7**.

The changes of the chemical shifts of the aromatic protons in unsubstituted [2$_n$]cyclophanes upon mono- and diruthenium complexation have already been documented.[3,4] In analogy, we observe differences between the aromatic three- and four-spin systems of **6** and **7** on the one and **9−13** on the other hand. In the complexes **9**, **11**, and **12**, the proton signals of the single deck bound to Ru$^{2+}$ move upfield ∼−0.5 ppm, whereas the signals of the unbound deck are shifted ∼+0.5 ppm downfield with respect to the signals of the free ligands. Complexation at both cyclophane decks results in very little upfield shift of the signals of the aromatic protons in **10** and **13** as compared to the free cyclophanes by a mutual compensation of the effects of both Ru$^{2+}$ units.

On the other hand, the change of chemical shifts for the vinyl protons upon complexation is rather drastic. Monocapping of **7** leads to only a slight downfield shift of the signal pattern for the vinyl protons attached to the unbound deck in **11** and **12** [H(17) and H(18a/b)]. The corresponding signals of H(19) and H(20a/b) (vinyl group at the ruthenium bound deck) are, however,

moved strongly toward each other. The upfield shift of the CH= proton, H(19), is less pronounced than the downfield shift of the =CH$_2$ protons, the latter being stronger for the *trans* [H(20a)] than for the *cis* [H(20b)] proton. In the biscapped diruthenium complex **13**, these effects are even more pronounced and the signals appear even further downfield. This influence of the complexation with Ru$^{2+}$ allows the distinction of the signals attributed to **9a** and **9b** in the mixture of the monocapped monovinyl complexes. Only in **9b** is the vinyl group bound to the deck attached directly to Ru$^{2+}$. Accordingly, the signals of protons H(17) and H(18a/b) are only separated by ∼0.3 ppm, while in **9a** the difference in the shift of the corresponding signals is >1 ppm.

As a general trend for the ethano protons H(1), H(2), H(9), and H(10), we observe a slight downfield shift upon complexation without being able to trace the individual signals.

**^{13}C NMR Spectra.** It is known from previous studies, that ^{13}C NMR spectra are much more sensitive to metal complexation than ^{1}H NMR spectra.[4,20,21] The ^{13}C NMR results for the cyclophane−ruthenium complexes described here follow this general behavior. They do largely reflect the trends described above for the ^{1}H NMR data. Additionally, however, they contain information about the influence of ruthenium complexation on the positions of the quaternary carbon signals in the cyclophane ligand.

In both the mono- and divinyl compounds, monocapping shifts the CH carbon signals of the ruthenium-bound deck −40 to −45 ppm upfield (**9**, **11**, **12**), whereas the CH carbon signals of the unbound deck appear +2−3 ppm downfield as compared to the free ligand. The CH carbon signals of the biscapped complexes **10** and **13** are shifted 1−2 ppm less upfield than those carbon signals of the bound deck in the monocapped species.

The signals of the quaternary carbons C(3), C(6), C(11), and C(14) that are connected to the ethano bridges are much less influenced by the complexation. Monocapping shifts the corresponding signals −5 to −8 ppm upfield, whereas the signals for the unbound deck move downfield by +1−2 ppm as compared to the free cyclophane. Biscapping results in an upfield shift of −9 to −10 ppm. These observations are in accordance with the single-crystal X-ray analysis of **11**, which shows that these carbons are directed away from the ruthenium atom, forming prow and stern of the boat-shaped cyclophane decks. This geometry results in longer carbon−ruthenium bond distances than in the case of the CH carbons (see also Table 2).

The changes for the chemical shift values of the vinyl group carbons caused by ruthenium complexation of the cyclophane arene decks are displayed in Figure 2. In the spectra of the free cyclophanes, the signals for the α- and β-carbons appear around 135 and 114 ppm, respectively, for both **6** and **7**, close to the values for styrene (137 and 113 ppm).[22] Monocapping of the aromatic deck opposite to the vinyl group moves the two

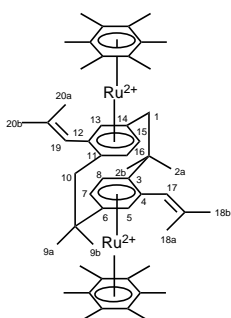(20) Chisholm, M. H.; Godleski, S. *Prog. Inorg. Chem.* **1976**, *20*, 299−419.

(21) Plitzko, K.-D.; Boekelheide, V. *Organometallics* **1988**, *7*, 1573−1582.

(22) Kalinowski, H.-O.; Berger, S.; Braun, S. *^{13}C-NMR-Spektroskopie*; Georg Thieme Verlag: Stuttgart, 1984; p 143.

**Table 3.  ¹H NMR Spectral Data of Ruthenium Cyclophane Complexes**

| compound | CH (position) | type | $J$ | CH₂ (position) | type | $J$ | CH₃ (position) | type |
|---|---|---|---|---|---|---|---|---|
| **6** | 6.78 (17) | dd | 17.4, 10.9 | 5.52 (18a) | dd | 17.4, 1.6 | | |
| | 6.70 (15) | dd | 7.8, 1.8 | 5.27 (18b) | dd | 10.9, 1.6 | | |
| | 6.53 (5) | d | 1.7 | 3.46 (2a) | ddd | 13.5, 10.0, 1.9 | | |
| | 6.51 (12) | dd | 7.8, 1.8 | 3.13−2.90 (1,9,10) | m | | | |
| | 6.48 (13) | dd | 7.8, 1.8 | 2.78 (2b) | ddd | 13.5, 10.4, 6.7 | | |
| | 6.46 (7) | dd | 7.7, 1.7 | | | | | |
| | 6.41 (8) | d | 7.7 | | | | | |
| | 6.38 (16) | dd | 7.8, 1.8 | | | | | |
| **9a** | 7.07 | d | 1.6 | 5.83 (18a) | dd | 17.4, 0.7 | 2.45 (HMB) | s |
| | 7.02 | m | | 5.50 (18b) | dd | 11.0, 0.7 | | |
| | 6.95−6.86 } (5,7,8) | *a* | | 3.84−3.77 (2a) | m | | | |
| | 6.90 (17) | dd | 17.4, 11.0 | 3.50−2.98 (1,2b,9,10) | m | | | |
| | 6.01 (15) | d | 6.5 | | | | | |
| | 5.93 (12,13) | s | | | | | | |
| | 5.86 (16) | d | 6.5 | | | | | |
| **9b** | 6.95−6.86 (12,13,15,16) | *a* | | 6.33 (18b) | d | 10.9 | 2.36 (HMB) | s |
| | 6.62 (17) | dd | 17.3, 10.9 | 6.32 (18a) | d | 17.3 | | |
| | 6.08 (5) | s | | 3.50−2.98 (1,2,9,10) | m | | | |
| | 5.97 (8) | d | 6.4 | | | | | |
| | 5.95 (7) | d | 6.4 | | | | | |
| **10** | 6.72 (17) | dd | 17.0, 11.0 | 6.56 (18a) | d | 17.0 | 2.51 (HMB-A) | s |
| | 6.54 (5) | s | | 6.49 (18b) | d | 11.0 | 2.41 (HMB-B) | s |
| | 6.41 (8) | d | 6.4 | 3.71−3.66 (2a) | m | | | |
| | 6.39 (13) | d | 6.6 | 3.55−3.48 } (1,2b,9,10) | m, 5H | | | |
| | 6.36 (12) | d | 6.6 | 3.40−3.35 | m, 2H | | | |
| | 6.35 (7) | d | 6.4 | | | | | |
| | 6.31 (16) | d | 6.5 | | | | | |
| | 6.28 (15) | d | 6.5 | | | | | |
| **7** | 6.80 (17,19) | dd | 17.4, 11.0 | 5.51 (18a,20a) | dd | 17.4, 1.3 | | |
| | 6.64 (7,15) | dd | 7.8, 1.6 | 5.27 (18b,20b) | dd | 11.0, 1.3 | | |
| | 6.54 (5,13) | d | 1.6 | 3.45 (2a,10a) | ddd | 13.5, 10.0, 2.6 | | |
| | 6.31 (8,16) | d | 7.8 | 3.24 (1b,9b) | ddd | 13.2, 10.7, 2.6 | | |
| | | | | 3.15 (1a,9a) | ddd | 13.2, 10.0, 5.8 | | |
| | | | | 3.01 (2b,10b) | ddd | 13.5, 10.7, 5.8 | | |
| **11** | 7.12 (5) | s | | 6.10 (20a) | d | 17.2 | | |
| | 6.96−6.89 } (4′,5′,7′,8′,17) | m | | 5.98 (20b) | d | 10.7 | | |
| | 6.82 (7,8) | d | 1.1 | 5.83 (18a) | dd | 17.4, 0.7 | | |
| | 6.58 (19) | dd | 17.2, 11.0 | 5.49 (18b) | dd | 11.0, 0.7 | | |
| | 6.24 (13) | d | 1.1 | 3.76 (2a) | | | | |
| | 6.02 (15) | dd | 6.3, 1.2 | 3.38−2.89 } (1,2b,9,10,1′,2′,9′,10′) | m | | | |
| | 5.86 { (12′,13′,15′,16′) | s | | | | | | |
| | 5.82 (16) | d | 6.4 | | | | | |
| **12** | 7.14 (5) | d | 1.9 | 6.34 (20b) | d | 11.0 | 2.36 (HMB) | s |
| | 6.96 (17) | dd | 17.4, 11.0 | 6.32 (20a) | d | 17.2 | | |
| | 6.88 (7) | dd | 7.9, 1.9 | 5.85 (18a) | d | 17.4 | | |
| | 6.83 (8) | d | 7.9 | 5.51 (18b) | d | 11.0 | | |
| | 6.64 (19) | dd | 17.2, 11.0 | 3.87−3.81 (2a) | m | | | |
| | 6.12 (13) | d | 1.1 | 3.44−3.00 (1,2b,9,10) | m | | | |
| | 6.01 (15) | dd | 6.4, 1.1 | | | | | |
| | 5.91 (16) | d | 6.4 | | | | | |

Downloaded by CARLI CONSORTIUM on June 30, 2009
Published on January 9, 1996 on http://pubs.acs.org | doi: 10.1021/om9504314

**Table 3 (Continued)**

| compound |  | $^1$H NMR chemical shift values and coupling constants *J* |  |  |  |  |  |  |  |
|---|---|---|---|---|---|---|---|---|---|
|  |  | CH (position) | type | *J* | $CH_2$ (position) | type | *J* | $CH_3$ (position) | type |
| **13** |  | 6.75 (17,19) | dd | 17.0, 11.0 | 6.58 (18a,20a) | d | 17.0 | 2.40 (HMB) | s |
|  |  | 6.61 (5,13) | s |  | 6.51 (18b,20b) | d | 11.0 |  |  |
|  |  | 6.37 (8,16) | d | 6.0 | 3.72−3.66 (2a,10a) | m |  |  |  |
|  |  | 6.29 (7,15) | d | 6.0 | 3.54−3.36 (1,2b,9,10) | m |  |  |  |

Ru2+
20a
20b
13
14
1
12
15
19
11
16
2a
10
8
2b
3
17
7
4
6
5
18b
9a
9b
Ru2+
18a

[a] Could not be determined due to signal overlap.


135,0
130,0
125,0
120,0
115,0
6
9a
9b
10
7
11
12
13
18
17
17
20
19
18
Compound
$^{13}$C NMR Chemical Shift / ppm
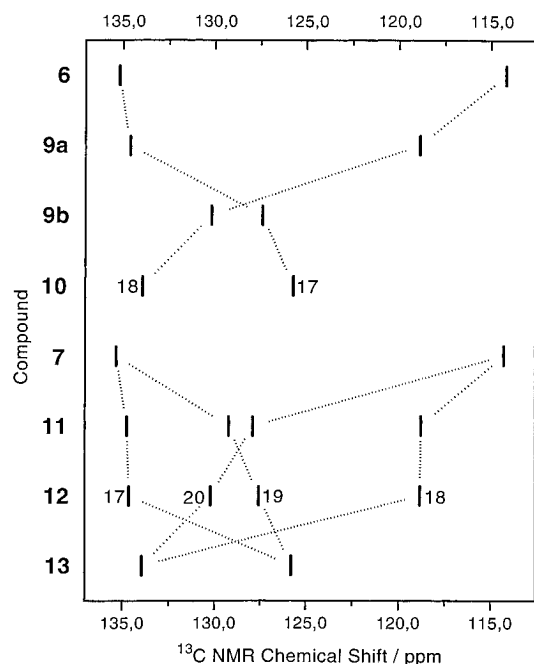
**Figure 2.** $^{13}$C NMR chemical shift values for the vinyl carbon atoms in the cyclophane ligands and their ruthenium complexes.

signals slightly toward each other [C(17), C(18) in **9a**, **11**, and **12**]. Monocapping of the cyclophane deck substituted by the vinyl group, however, causes a drastic change in the chemical shift values of both carbons [C(17), C(18) in **9b** and C(19), C(20) in **11** and **12**]. The α-carbon signal moves upfield more than −7 ppm, whereas the β-carbon signal shifts downfield +16 ppm, resulting in a crossover of the signal positions. Biscapping enhances this effect. In the spectra of **10** and **13**, the α-carbon signals appear more than −9 ppm upfield, while the β-carbon signals are shifted downfield almost +20 ppm from the positions of the corresponding signals of the free ligands.

The "disturbed" vinyl groups are not directly bound to the ruthenium atom, as shown by the X-ray results discussed above. The changes of the chemical shift values can, however, be explained by electronic effects exerted by the ruthenium-bound cyclophane deck. The chemical shift of the α-carbon in substituted ethylenes is mainly influenced by the electronegativity of the substituent, while the chemical shift of the β-carbon can generally be explained by the contribution of polar resonance structures of the system.[23] Hence, the −M-effect of the ruthenium-capped deck should be largely responsible for the chemical shift changes of the β-vinyl carbons in our complexes. For the α-vinyl carbon, not only −I- but also ring current effects of the cyclophane decks have to be considered. Since ruthenium complexation decreases the ring current, this could be the reason for the smaller upfield shift of the α-vinyl carbon signal as compared to the larger downfield shift of the signal of the β-vinyl carbon.

Thus, the changes in the $^1$H and the $^{13}$C NMR behavior of the vinyl groups in complexes **9**−**13** can be explained by the delocalization of positive charge from the ruthenium cyclophane moiety onto the vinyl group, thereby reducing the electron density in the substituent.

**Electrochemical Studies.** Preliminary experiments showed that the ruthenium complexes discussed here are stable in propylene carbonate (PC) in both the Ru(II) and the Ru(0) oxidation state. This solvent was therefore used almost exclusively for the electrochemical study of these compounds. Due to its good solubility **11** could also be studied in dichloromethane. The cyclophane ligands were investigated in acetonitrile and in PC, but no difference in their general electrochemical behavior was found in these two solvents.

The electrochemical reduction of the vinyl compounds **9**−**13** was investigated by cyclic voltammetry and chronocoulometry at platinum and glassy carbon disk electrodes. Cyclic voltammetry and bulk coulometric experiments with **9**, **11**, and **12** revealed chemically reversible two-electron reductions similar to those of the unsubstituted complexes **1** and **2**.[5,6,24] Also, **10** and **13** show the same general electrochemical behavior in cyclic voltammetry upon reduction as their unsubstituted analogue **3**:[8] a two-electron process accompanied by a fast chemical follow-up reaction. All vinyl-substituted complexes, with the exception of **11**, however, additionally exhibit potential- and time-dependent adsorption phenomena at both electrode materials. This was confirmed by chronocoulometric measurements. The detailed analysis of such behavior requires additional electrochemical experiments whose results will be reported elsewhere.

The vinylcyclophanes **6** and **7** themselves do not show any reduction peaks in the accessible potential range (cathodic limit in $CH_3CN$ is ∼−2.4 V; all potentials in

---

(23) See p 215 ff. in ref 22.

(24) Krauss, B.; Speiser, B. Unpublished results.

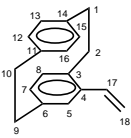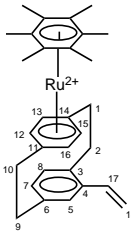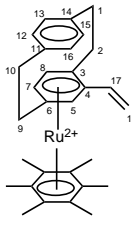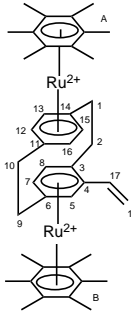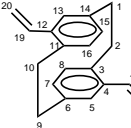**Table 4. $^{13}$C NMR Spectral Data of Ruthenium Cyclophane Complexes**[a]
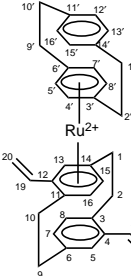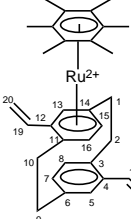
| compound | $^{13}$C NMR chemical shift values (position assignments) | | | |
|---|---|---|---|---|
| | quaternary | tertiary | secondary | primary |
| **6** | 139.78 (6)<br>139.31 (11,14)<br>137.90 (3)<br>137.77 (4) | 135.18 (17)<br>134.73 (8)<br>132.99 (12,13)<br>131.91 (7)<br>131.78 (16)<br>130.12 (5)<br>129.53 (15) | 114.19 (18)<br>35.44 (10)<br>35.19 (9)<br>34.63 (1)<br>33.63 (2) | |
| **9a** | 141.74 (4)<br><br>141.46 (6)<br><br>139.00 (3)<br>131.14 }(11 & 14)<br>131.03<br>109.27 (HMB) | 137.27 (8)<br><br>135.37 (7)<br><br>134.60 (17)<br>131.58 (5)<br><br>91.53 }(12 & 13)<br>91.44<br>90.28 (16)<br>88.73 (15) | 118.87 (18)<br>34.70 }(1 & 9 & 10)<br>32.05<br>31.48<br>32.88 (2) | 17.96 (HMB) |
| **9b** | 141.22 }(11 & 14)<br>140.84<br><br>131.17 }(3 & 6)<br>129.07<br><br>108.95 (HMB)<br>99.30 (4) | 135.58 }(12 & 13)<br>135.37<br><br>134.41 (16)<br><br>133.18 (15)<br>127.39 (14)<br>93.11 (7)<br>90.92 (8)<br>85.69 (5) | 130.18 (18)<br><br>34.96<br>34.00 }(1 & 2 & 9 & 10)<br>31.83<br>30.91 | 17.54 (HMB) |
| **10** | 131.38 (11)<br>130.95 (6)<br>130.72 (14)<br><br>127.90 (3)<br>111.32 (HMB-A)<br>110.85 (HMB-B)<br>101.61 (4) | 125.69 (17)<br>94.34 (8)<br>92.61 }(12 & 13)<br>92.52<br>91.88 (7)<br>91.48 (16)<br>90.50 (15)<br>86.30 (5) | 133.92 (18)<br>31.55 (10)<br>31.17 (9)<br><br>30.43 (1)<br>30.18 (2) | 18.11 (HMB-A)<br>17.66 (HMB-B) |
| **7** | 139.38 (6,14)<br>137.74 (3,11)<br>137.71 (4,12) | 135.33 (17,19)<br>133.43 (8,16)<br>130.11 (5,13)<br>129.31 (7,15) | 114.29 (18,20)<br>34.24 (1,9)<br>32.99 (2,10) | |
| **11** | 141.63 (4)<br>141.07 (14′,11′)<br><br>140.76 (6)<br>138.73 (3)<br>133.49 (3′,6′)<br>132.88 (14)<br>131.92 (11)<br><br>97.60 (12) | 135.98 (8)<br>135.58 }(12′,13′ & 15′,16′)<br>135.51<br>134.75 (17)<br>132.16 (7)<br>131.29 (5)<br>129.22 (19)<br>88.39 }(4′,5′ & 7′,8′)<br>87.40<br>88.36 (16)<br>84.28 }(13 & 15)<br>84.27 | 127.90 (20)<br>118.78 (18)<br><br>34.96 (1′,10′)<br>34.18 (9)<br>32.86 (2′,9′)<br>32.85 (2)<br>31.94 (1)<br><br>31.35 (10) | |
| **12** | 141.54 (4)<br>140.92 (6)<br>139.03 (3)<br>131.01 (14)<br>129.20 (11)<br>109.05 (HMB)<br>99.42 (12) | 135.91 (8)<br>134.64 (17)<br>132.36 (7)<br>131.49 (5)<br>127.57 (19)<br>92.20 (16)<br>88.80 (15)<br>85.84 (13) | 130.21 (20)<br>118.83 (18)<br>33.91 (9)<br>32.64 (2)<br>31.09 (1)<br>30.48 (10) | 17.52 (HMB) |

**Table 4 (Continued)**

| compound | $^{13}C$ NMR chemical shift values (position assignments) | | | |
|---|---|---|---|---|
| | quaternary | tertiary | secondary | primary |
| **13** | 130.45 (6,14)<br>128.31 (3,11)<br>111.01 (HMB)<br>101.52 (4,12) | 125.79 (17,19)<br>93.24 (8,16)<br>90.04 (7,15)<br>86.34 (5,13) | 133.94 (18,20)<br>30.18 (1,9)<br>30.05 (2,10) | 17.67 (HMB) |
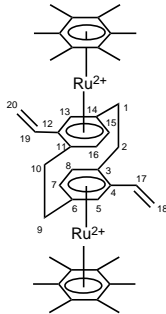
*a* Position assignments separated by "&" could not be determined for individual carbon atoms.
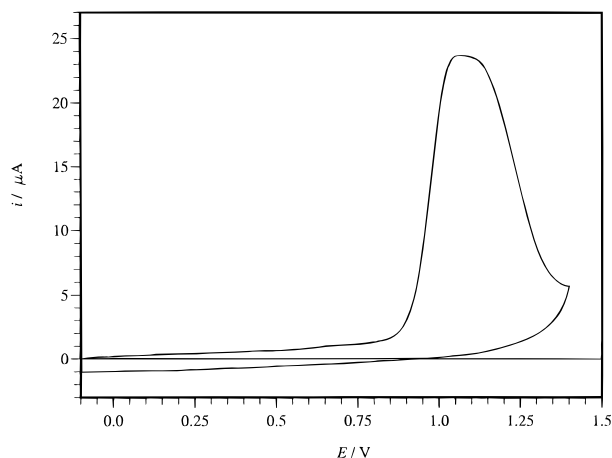


**Figure 3.** Cyclic voltammogram of **7** in 0.1 M TBAHFP/
CH$_3$CN at a Pt disk electrode: $c = 4 \times 10^{-4}$ M; $\nu = 0.05$
V·s$^{-1}$.



**Figure 4.** Background-subtracted cyclic voltammogram
of **11** in 0.1 M TBAHFP/CH$_2$Cl$_2$ at a Pt disk electrode: $c =
5 \times 10^{-4}$ M; $\nu = 0.1$ V·s$^{-1}$.

this work are referenced vs the ferrocene/ferrocenium
standard redox couple[25]). On the other hand, they can
be electrochemically oxidized in a chemically irreversible
process (peak potential $E_p^{ox} \approx 1.05$ V; Figure 3 for the
case of **7**).

Repeated potential cycling in acetonitrile or PC leads
to formation of a dielectric polymer film, which succes-
sively blocks the electrode surface. This is evident from
a decrease of the peak current during multicycling: In
a second scan, the oxidation peak of **7** has totally
disappeared. With **6** at comparable concentrations, it
takes ~10 cycles until the oxidation peak has vanished.
The film formation also explains the shape of the
current/potential curve in Figure 3, which decreases
after the peak much faster than expected for a diffusion-
controlled wave. The film is stable and the modified
electrode can be transferred into monomer-free electro-
lytes. Characterization of the poly(vinylcyclophane)-
modified electrodes will be described elsewhere.

The unsubstituted [2$_2$]paracyclophane can also be
oxidized *electrochemically.*[26] In this case, oxidation of
the cyclophane system at more positive potentials
($E_p^{ox} = 1.15$ V under our conditions). The detailed
mechanism of the electrode reaction, however, is not yet
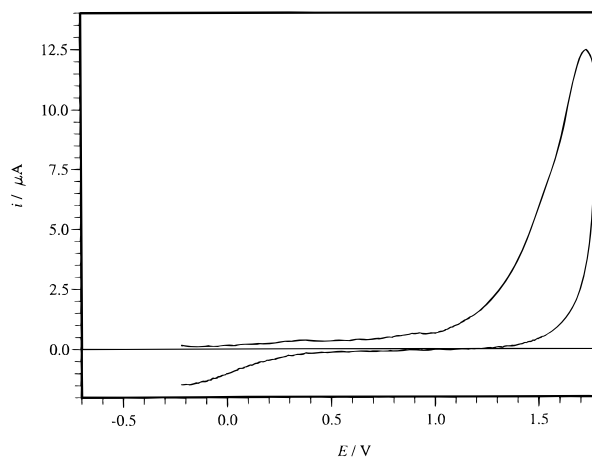known. In a recent paper, Adam and co-workers

showed that *chemical* oxidation of [2$_2$]paracyclophane
leads to cleavage of the carbon–carbon bond in one of
the ethano bridges and further chemical reactions of the
resulting open-chain radical cation.[27] In contrast to the
case of this unsubstituted parent molecule, but in
analogy to the electrochemical polymerization of sty-
rene,[10] we assume that oxidation of **6** and **7** results in
polymerization reactions involving the vinyl groups of
radical cations **6**·$^+$ and **7**·$^+$ and the respective parent
molecules (**6** and **7**).

Cyclic voltammograms of the monoruthenium vinyl-
cyclophane complexes **9a**, **9b**, **11**, and **12** also show
oxidation peaks. As compared to those of the free
ligands, they are shifted more than 0.5 V to more
positive potentials (Figure 4) and appear close to the
anodic limit (~1.8 V for CH$_2$Cl$_2$) of the electrolyte. A
plot of $i_p$ vs $\nu^{1/2}$ for the case of **11** is linear, indicating
that the redox reaction of adsorbed molecules does not
contribute to the current significantly. The peak cur-
rents of the chemically irreversible anodic *oxidations*
can thus be compared to those of the corresponding two-
electron *reductions*, if we consider only cases where the
influence of adsorption on the peaks of the latter is
small. The oxidation peaks have roughly half the size
of the reduction peaks. In the case of the mixture of
**9a** and **9b**, the peak height of the *oxidation* corresponds

(25) Gritzner, G.; Kůta, J. *Pure Appl. Chem.* **1984**, *56*, 461–466.
(26) Sato, T.; Torizuka, K. *J. Chem. Soc., Perkin Trans. 2* **1978**,
1199–1204.

(27) Adam, W.; Miranda, M. A.; Mojarrad, F.; Sheikh, H. *Chem. Ber.*
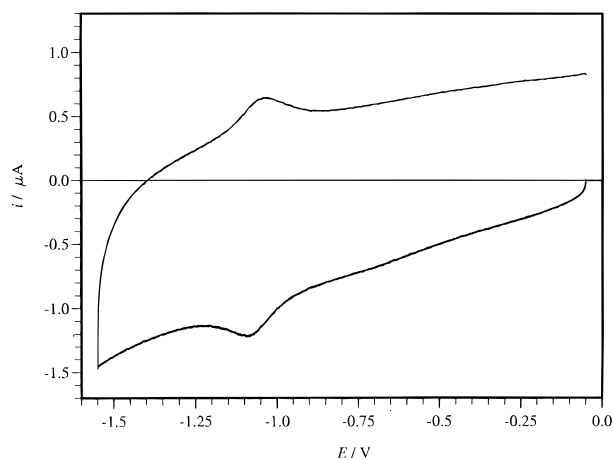**1994**, *127*, 875–879.

**Figure 5.** Cyclic voltammogram of a modified glassy carbon disk electrode in 0.1 M NaBPh$_4$/PC, $\nu = 0.1$ V·s$^{-1}$; modification by two potential cycles in $5 \times 10^{-3}$ M solution of **12** in 0.1 M TBAHFP/PC at $\nu = 0.05$ V·s$^{-1}$; surface excess concentration $\Gamma \approx 2.5 \times 10^{-11}$ mol·cm$^2$, calculated from charge under the reduction peak.

to half of the height of the *reduction* peak attributed to isomer **9a**. Thus, the anodic oxidations are *one*-electron transfers.

Experiments at concentrations higher than $10^{-3}$ M again show that material is deposited on the electrode surface. Potential cycling over the oxidation waves of **9a**, **11**, and **12** at these concentrations leads to formation of redox-active films on the electrode. The cyclic voltammogram of such a modified electrode in an electrolyte solution without monomer is shown in Figure 5. The signals are unsymmetric with steeper falling than rising parts. The peak currents are proportional to $\nu$. Thus, indeed surface-confined species undergo electron transfer.[28] The full peak width at half-maximum ($E_{\text{fwhm}}$ $\approx 180$ mV at $\nu = 0.1$ V·s$^{-1}$) is much larger than the theoretical value of 45.3 mV expected for a two-electron transfer.[28] This can be explained by strong repulsive interactions between the doubly charged ruthenium centers and/or slow heterogeneous charge transfer. Slow heterogeneous kinetics have been reported for the structurally closely related bis($\eta^6$-hexamethylbenzene)-ruthenium(II) dication.[29] Again, the detailed characterization of these redox-active films will be published elsewhere.

For complexes **3**, **9b**, and **10**, no oxidation peaks appear within the potential range accessible in PC (anodic limit $\sim+1.9$ V). Complex **2** on the other hand, exhibits a chemically irreversible oxidation at the very end of the solvent window ($E_{\text{p}}^{\text{ox}} \approx +1.85$ V).

From the oxidation potentials, it is evident that the highest occupied molecular orbitals (HOMOs) of **9a**, **11**, and **12** lie energetically much higher than those of **9b** or **10**, for which no oxidation is found in the accessible potential range. According to the NMR data in these latter complexes, only vinyl groups are present which are bound to ruthenium-capped cyclophane decks and bear considerable positive charge. Only if undisturbed vinyl groups (bound to uncomplexed cyclophane decks) are present, the HOMO lies high enough to be accessible

to electrochemical oxidation. This in turn indicates that the atomic orbitals of the vinyl substituents largely contribute to the HOMO of the complexes.

Comparison of the *reduction* potentials of **2** [$E°$(I) = $-0.897$ V, $E°$(II) = $-0.975$ V][24] and **11** ($E° = -0.930$ V) reveals that the presence of two vinyl groups has only little influence on the potentials of the metal-centered two-electron reductions. The *oxidation* peak potential of **2** on the other hand appears more than 0.3 V more positive than those of **9a**, **11**, and **12**. In contrast to **11**, no (undisturbed) vinyl groups bound to uncomplexed cyclophane decks are present in **2**. Thus, a HOMO with lower energy results in the latter compound and oxidation is more difficult than for **11**.

## Conclusions

The results reported in this paper show that mono- and diruthenium complexes of vinylcyclophanes can be prepared by a modification of Bennett's capping procedure, without the use of TFA. The crystal structure of **11** demonstrates that there is no direct bonding interaction between the vinyl groups and the ruthenium atom. NMR data on the other hand indicate that ruthenium complexation has a marked electron-withdrawing effect on vinyl groups directly bound to capped cyclophane decks, while this effect is much smaller for vinyl groups attached to noncomplexed decks. This is also evident from electrochemical investigations, where anodic oxidations can only be found for such complexes that bear vinyl groups at uncapped cyclophane decks. Electrochemical oxidation of the vinylcyclophanes results in formation of dielectric polymer films on the electrode. The oxidation of vinyl-substituted ruthenium complexes at concentrations higher than $10^{-3}$ M leads to the formation of redox-active films of vinyl-polymerized metallocenes on the electrode surface. The first steps of the proposed electrochemical solid phase synthesis of stacked polymetallocenes have thus been accomplished.

## Experimental Section

**General Comments.** Electrospray mass spectra of the ruthenium compounds were measured on an API III spectrometer with an electrospray (ion spray) source (Sciex, Thornhill, ON, Canada) at an orifice voltage of $\sim$50 V.[30] Acetone or nitromethane were used as solvent. Elemental analyses were determined by the Mikroanalytisches Laboratorium der Universität Tübingen. The ruthenium complexes melt with decomposition, giving a melting behavior that is not useful for characterization and so is not reported.

**Syntheses. (R,S)-4-Ethenyl[2$_2$](1,4)cyclophane (6)** was prepared according to a literature procedure.[12]

**(R,S)-(11-16-$\eta^6$-4-Ethenyl[2$_2$](1,4)cyclophane)($\eta^6$-hexamethylbenzene)ruthenium(II) Bis(tetrafluoroborate) (9a) and (R,S)-(3,8-$\eta^6$-4-ethenyl[2$_2$](1,4)cyclophane)($\eta^6$-hexamethylbenzene)ruthenium(II) Bis(tetrafluoroborate) (9b).** A mixture of 830 mg (4.26 mmol) of silver tetrafluoroborate and 712.5 mg (1.065 mmol) of bis(hexamethylbenzene)dichlorobis($\mu$-chloro)diruthenium(II)[31] in 5 mL of acetone was stirred at room temperature for 30 min. The resulting precipitate of silver chloride was removed by filtration and washed with acetone until the washings were clear and colorless. After

(28) Murray, R. W., Ed. *Molecular Design of Electrode Surfaces*; Techniques of Chemistry 22; Wiley: New York, 1992.
(29) Pierce, D. T.; Geiger, W. E. *J. Am. Chem. Soc.* **1992**, *114*, 6063–6073.

(30) Schmeer, K. Dissertation Universität Tübingen, Tübingen, Germany, 1995.
(31) Bennett, M. A.; Matheson, T. W.; Robertson, G. B.; Smith, A. K.; Tucker, P. A. *Inorg. Chem.* **1980**, *19*, 1014–1021.

concentration of the combined filtrate and washings to a volume of ~10 mL, 499 mg (2.13 mmol) of **6** was added. The mixture was boiled under reflux for 90 min, while the color changed from orange to tan. After the mixture had cooled, the resulting precipitate was collected by filtration and washed with 10 mL of acetone. The yellowish green solid was dried under vacuum to give 1.270 g (89%) of a 2:1 mixture of **9a** and **9b** (ratio determined by integration of the $^1$H NMR signals of the hexamethylbenzene ligand in both isomers). Attempts to separate **9a** from **9b** by fractional crystallization failed. MS (electrospray): $m/e$ found for $C_{30}H_{36}RuBF_4^+$ [$M^{2+}$ + $BF_4^-$], 580.3, 581.3, 582.3, 583.3, 584.3, 585.3 (100), 586.3, 587.3, 588.3, 589.3, $M^{2+}$, 246.2, 246.7, 247.2, 247.7, 248.2, 248.7, 249.2 (90), 249.7, 250.2, 250.7, 251.2 (both experimental isotope distribution patterns matched precisely the calculated ones with respect to both signal and intensity). For NMR data, see Tables 3 and 4.

Compound **12** was prepared similarly following this procedure. Yield: 260 mg (83%). Anal. Calcd for $C_{32}H_{38}RuB_2F_8$: C, 55.12; H, 5.49. Found: C, 54.94, H, 5.46. For NMR data, see Tables 3 and 4.

**(R,S)-($\eta^6$,$\eta^6$-4-Ethenyl[2$_2$](1,4)cyclophane)bis($\eta^6$-hexamethylbenzene)diruthenium(II,II) Tetrakis(tetrafluoroborate) (10).** A mixture of 2.147 g (11.02 mmol) of silver tetrafluoroborate and 1.843 g (2.76 mmol) of ($\eta^6$-hexamethylbenzene)dichlorobis($\mu$-chloro)diruthenium(II) in 10 mL of acetone was stirred for 30 min at room temperature. The resulting precipitate of silver chloride was collected by filtration and washed with acetone until the washings were clear and colorless. After concentration of the combined filtrate and washings to a volume of ~15 mL, 129 mg (0.55 mmol) of **6** was added. The mixture was boiled under reflux for 2.5 h. After the mixture had cooled, the resulting precipitate was collected by filtration, washed with 5 mL of acetone, dissolved in nitromethane, and reprecipitated by addition of ether. The precipitate was again collected by filtration and dried under vacuum. Yield: 210 mg (35%). MS (FAB): $m/e$ calcd for $C_{42}H_{54}{}^{102}Ru_2B_3F_{12}^+$ 1022.2, found 1022.4. For NMR data, see Tables 3 and 4.

Compound **13** was prepared similarly following this procedure. Yield: 120 mg (27%). MS (electrospray): $m/e$ calcd for $C_{44}H_{56}Ru_2^{3+}$ 262.7, found 262. For NMR data, see Tables 3 and 4.

**(R,S)-($\eta^6$-[2$_2$](1,4)Cyclophane)(11-16-$\eta^6$-4,12-diethenyl-[2$_2$](1,4)cyclophane)ruthenium(II) Bis(tetrafluoroborate) (11).** A mixture of 145 mg (0.74 mmol) of silver tetrafluoroborate and 142 mg (0.186 mmol) of di-$\mu$-chlorobis-[($\eta^6$-[2$_2$](1,4)cyclophane)chlororuthenium(II)] in 5 mL of acetone was stirred for 1 h at room temperature. The resulting precipitate of silver chloride was collected by filtration and washed with acetone until the washings were clear and colorless. After concentration of the combined filtrate and washings to a volume of ~10 mL, 96.5 mg (0.37 mmol) of **7** was added. The mixture was boiled under reflux for 5.5 h. After the mixture had cooled, it was diluted with 100 mL of ether and the resulting precipitate was collected by filtration and dried under vacuum. The $^1$H NMR spectra of this material showed it to be a mixture of at least three components. Therefore the material was dissolved in 50 mL of acetone and insoluble solids were removed by filtration. The flask with the filtrate was placed in a tank with diisopropyl ether. After 1 week, yellow crystals had formed at the glass wall of the flask besides some dark amorphous material. The crystals were removed from the glass wall and collected by filtration. The single-crystal X-ray structure analysis shows the presence of one molecule of acetone per molecule of **11**. Yield: 80 mg (29%). MS (electrospray): $m/e$ found for $C_{36}H_{36}RuBF_4^+$ [$M^{2+}$ + $BF_4^-$], 651.4, 652.4, 653.4, 654.4, 655.4, 656.4, 657.4, 658.4, 659.4, 660.4, $M^{2+}$, 282.3, 282.8, 283.3, 283.8, 284.3, 284.8, 285.3, 285.8, 286.3, 286.8, 287.3 (both experimental isotope distribution patterns matched precisely the calculated ones

with respect to both signal and intensity). For NMR data, see Tables 3 and 4.

**Polymerization of 6 in TFA.** A mixture of 50 mg of **6** and 5 mL of TFA was refluxed for 3 h. It was cooled to room temperature and the acid removed under vacuum. The remaining solid was taken up in ~20 mL of acetone and precipitated by addition of water. The tan solid was collected by filtration and dried at room temperature under vacuum. Yield: 45 mg.

**X-ray Measurement.** Data were collected on an Enraf-Nonius CAD4 diffractometer with Mo Kα ($\lambda$ = 0.709 30 Å) radiation. The structure was solved by Patterson methods (SHELX86)[32] and refined with all data on $F^2$ with a weighting scheme of $\omega^{-1} = \sigma^2 (F_o^2) + (aP)^2 + bP$ with $P = (F_o^2 + 2F_c^2)/3$ using SHELXL-93.[33] Non-hydrogen atoms were refined anisotropically. All hydrogen atoms were included in calculated positions with common thermal parameters.

**NMR Experiments.** NMR spectra were measured on a Bruker AMX400 (400 MHz) or a Bruker AMX600 (600 MHz) spectrometer with standard techniques and programs supplied by Bruker. C,H correlations were performed using the HMQC sequence[34] preceded by a BIRD pulse to suppress signals from protons bound to $^{12}$C and to alleviate dynamic range problems.[35] A sensitivity-enhanced HSQC experiment[36] was carried out with **6**. Heteronuclear long-range correlation (HMBC) was optimized for coupling constants of 8 Hz with low-pass $J$ filter to suppress one-bond correlations.[37] Data extraction and analyses of NMR spectra were performed with the XSPEC software package (Version 2.0, Bruker Instruments Inc. & Spectrospin AG) running on an IRIS Indigo workstation (Silicon Graphics). Spectra of the ligands **6** and **7** and the polymerization product of **6** were measured in CDCl$_3$, while CD$_3$NO$_2$ was used for those of the ruthenium complexes. Chemical shift values ($\delta$) are reported in ppm relative to TMS using the residual solvent resonance as an internal reference (CDCl$_3$: $^1$H $\delta$ = 7.24 ppm, $^{13}$C $\delta$ = 77.00 ppm. CD$_3$NO$_2$: $^1$H $\delta$ = 4.33 ppm, $^{13}$C $\delta$ = 62.80 ppm). Coupling constants ($J$) are given in hertz.

**Electrochemical Experiments.** Cyclic voltammetry and chronocoulometry data were acquired with gas-tight full-glass cells, manufactured by the glass blowers of the Chemisches Zentralinstitut der Universität Tübingen. The cells can be connected to a high-vacuum/argon line. Acetonitrile (commercial grade) was distilled from P$_2$O$_5$, NaH, and again P$_2$O$_5$. It was passed over a column with Al$_2$O$_3$ (neutral, Brockmann activity I) and finally degassed by three freeze−pump−thaw cycles. Propylene carbonate (anhydrous, Aldrich, or distilled in glass, Burdick & Jackson) was distilled in vacuo (10$^{-1}$ Torr, 50 cm column with Raschig rings), fractionated, and degassed by three freeze−pump−thaw cycles. It was then transferred with needles and Teflon tubing onto highly activated Al$_2$O$_3$ (450 °C, 10$^{-5}$ Torr) at liquid nitrogen temperature, allowed to warm to room temperature, and transferred into a measuring flask containing supporting electrolyte. From there it was transferred into the electrochemical cell. Dichloromethane (commercial grade) was distilled from P$_2$O$_5$ and then from K$_2$-CO$_3$. It was degassed at the high-vacuum line with three freeze−pump−thaw cycles and condensed under high vacuum onto highly activated Al$_2$O$_3$ and then into ampules containing supporting electrolyte. These ampules were connected to a high-vacuum electrochemistry cell,[38] and the supporting electrolyte solution was transferred into the cell by tipping. The

(32) Sheldrick, G. M. *Acta Crystallogr., Sect. A* **1990**, *46*, 467−473.
(33) Sheldrick, G. M. *SHELXL-93, Programm for Crystal Structure Refinement*; University of Göttingen, Göttingen, Germany, 1993.
(34) Summers, M. F.; Marzilli, L. G.; Bax, A. *J. Am. Chem. Soc.* **1986**, *108*, 4285−4294.
(35) Bax, A.; Subramanian, S. *J. Magn. Reson.* **1986**, *67*, 565−569.
(36) Schleucher, J.; Schwendinger, M.; Sattler, M.; Schmidt, P.; Schedletzky, O.; Glaser, S. J.; Sørensen, O. W.; Griesinger, C. *J. Biomol. NMR* **1994**, *4*, 301−306.
(37) Bax, A.; Summers, M. F. *J. Am. Chem. Soc.* **1986**, *108*, 2093−2094.

supporting electrolytes were $n$-Bu$_4$NPF$_6$ (TBAHFP), prepared and purified according to a literature procedure,[39] and sodium tetraphenylborate (Fluka, puriss. p.a.), purified as described in the literature.[39] Both were used in 0.1 M concentration throughout. The working electrodes were Pt [3 mm diameter, Metrohm or Bioanalytical Systems (BAS)] and glassy carbon disks (3 mm diameter, BAS), polished with 0.05 $\mu$m alumina (BAS) prior to all experiments (electroactive area $A \approx 0.07$ cm$^2$). The reference electrode was a Ag/Ag$^+$ dual-reference electrode system with a Haber–Luggin capillary as described.[40] All potentials are recalibrated to the ferrocene/ferrocenium ion standard[25] in the respective solvent determined in separate experiments. A Pt wire served as auxiliary

electrode. Data were collected on a BAS 100B/W electrochemical workstation.

**Supporting Information Available:** Tables of crystallographic and structure refinement data, atomic coordinates and isotropic displacement parameters, bond lengths and angles, anisotropic displacement parameters, and hydrogen coordinates (8 pages). Ordering information is given on any current masthead page.

OM9504314

(38) Mills, J. L.; Nelson, R.; Shore, S. G.; Anderson, L. B. *Anal. Chem.* **1971**, *43*, 157–159.

(39) Salbeck, J. Dissertation, Universität Regensburg, Regensburg, Germany, 1988.

(40) Gollas, B.; Krauss, B.; Speiser, B.; Stahl, H. *Curr. Sep.* **1994**, *13*, 42–44.